ON THE OPTIMAL CELL SIZE IN A SENSOR NETWORK AIDED COGNITIVE RADIO SYSTEM

Pål Grønsund (Telenor, Fornebu, Norway; pal.gronsund@telenor.com; Department of Informatics, University of Oslo, Norway; paalrgr@ifi.uio.no); Ole Grøndalen (Telenor, Fornebu, Norway; ole.grondalen@telenor.com)

ABSTRACT

To exploit spectrum resources on a secondary basis, a Sensor Network Aided Cognitive Radio Network uses a wireless sensor network that assists a secondary cognitive radio network by providing information about the current primary spectrum occupancy. In this paper we aim to find the optimal cell size for the secondary network that exploits spectrum holes identified by the wireless sensor network. The secondary base station is deployed co-located with a mobile primary network that uses a cellular reuse pattern with seven frequencies. Performance of the secondary system and impact on the primary system is mainly studied in terms of throughput, packet loss and coverage when using spectrum holes in the space, time and frequency domains. Especially, we find that the cell size and configured transmit powers for the secondary system is important for optimal system performance, and that smaller cell sizes and less expensive base stations for the secondary system is beneficial. The impact on primary system performance was found to be low, but that optimal tuning of the sensor network is important.

1. INTRODUCTION

Cognitive radio (CR) and spectrum sensing are considered as promising concepts to exploit the spectrum resources more efficiently by dynamically utilizing radio spectrum not utilized by primary networks, referred to as spectrum holes. A wireless sensor network (WSN), not necessarily embedded in the CR, can be deployed to detect spectrum holes and report to the secondary system as proposed in the EU FP7 project SENDORA [1],[2]. In this paper we will refer to the SENDORA system as a Sensor Network Aided Cognitive Radio system where the secondary CR system uses a WSN to detect spectrum holes. Input on real time spectrum monitoring by using a separate low cost WSN was recently also requested by FCC [3].

In [4], we studied the system level performance of an example SENDORA system for different secondary cell sizes. A total performance study of the SENDORA system is complex to achieve with analytical modelling, hence the system level simulator ns-2 was used. In this paper we build on that work and present an elaborative and complete study. All parts of the SENDORA system are implemented in the simulator; a primary network, a centralized secondary network, a WSN and a centralized fusion centre (FC). The FC aggregates spectrum measurements from the sensors and allocates a channel to the secondary network. Furthermore, to get a detailed picture of performance we implement realistic network topologies, traffic models and the whole protocol stack of the secondary and primary systems with actual transport, network, link and physical layers.

In [5] we found that a high degree of co-location of secondary and primary base stations (BSs) is very important in order to achieve a positive business case for a SENDORA system. Therefore the main focus of this study is to determine the optimal cell-size and transmit power levels for the secondary network when co-located with a primary network. A realistic network scenario is considered where the primary network uses a cellular reuse pattern with seven frequencies.

Achievable rate for point-to-point communication using a potential spectrum hole in a frequency planned primary network was studied in [6] by using monte-carlo simulations. It was found that spectrum holes get saturated quite fast due to interference among cognitive users. Similar studies were performed in [7] for a single cell and in [8] for a frequency planned network. These works assumed a reduction in primary cell size as a compromise for the primary system to allow secondary users (SUs) and that the SUs can perfectly judge the distance to the primary users (PUs). In this paper, we consider a point-to-multipoint network, a realistic channel model and the PUs are mobile such that the considered spectrum holes [9] change dynamically in time and space. An interference requirement to allow secondary operation uses a constraint on interference at the PU [10]-[12], estimated by the FC by querying the WSN for presence of PUs.

The main focus and contribution of this paper is on finding the optimal cell size of the secondary network and on estimation of realistic network performance in a SENDORA system by simulations and on how spectrum holes can be exploited while respecting primary system interference constraints. Impact on the primary system performance will also be studied. The main performance metrics are throughput, packet loss and coverage. Though the WSN is a core component of the system and is implemented with energy detectors deployed in a rectangular grid, the main focus of this paper will not be on WSN performance. It should also be noted that the objective of this paper is not on optimization of algorithms.

The organization of the rest of this paper is as follows: Section 2 gives an overview of the SENDORA system. The network scenario considered is described and the necessary parameters and constraints are derived in Section 3. In section 4, we present and motivate the simulation scenarios that will be studied in detail. An analytical estimation of service range and coverage is given in Section 5 before the simulation results and performance evaluation are presented in Section 6. Finally, the paper is concluded in Section 7.

2. SENSOR NETWORK AIDED COGNITIVE RADIO SYSTEM

Figure 1 gives an overview of the SENDORA system consisting of four main parts; the primary network which in this case is WiMAX, the secondary network which in this case is a modified version of WiMAX with SENDORA functions implemented, the WSN and the centralized FC.

To get a channel allocation, the secondary network consults the FC which has the total responsibility for communicating with the WSN. The FC then allocates an available channel to the secondary system based on sensing results. The simulation model for the primary and secondary networks uses an ns-2 implementation of WiMAX [13] developed in WiMAX Forum. The FC and WSN are also implemented in ns-2. Each part of the SENDORA system will be described in the sequel of this section.

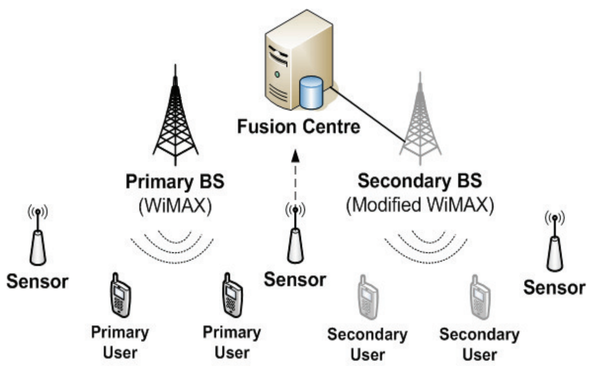

Figure 1 System Model

2.1. Primary System

To simulate the primary system, we use the WiMAX ns-2 model developed in WiMAX Forum which is based on the IEEE 802.16e [14] standard. The model includes a very detailed model of the MAC and also a good model of the PHY layers. The main parameters given in Table 1 are common for the primary and secondary systems. WiMAX uses orthogonal frequency division multiple access (OFDMA) and time division duplex (TDD) with 5 milliseconds OFDMA frames. Operating frequency is in the 2 GHz band and the channel bandwidth is 10 MHz with a total of 1024 subcarriers.

Table 1 System and OFDMA Parameters for primary and secondary systems

Parameter	Value
Frequency	2 GHz
Channel Bandwidth	10 MHz
FFT Size	1024
Duplexing	Time Division Duplex (DTT)
OFDMA Frame duration	5 ms
DL:UL ratio	2:1
Modulation types	BPSK, QPSK, 16-QAM, 64-QAM
FEC rates	1/2, 2/3, 3/4
Cyclic prefix mode	1/4
OFDM mapping	Vertical striping
Subcarrier allocation	Partially used subcarrier allocation
Total subcarriers used	840
Guard + null subcarriers	184
Pilot subcarriers	DL: 120, UL: 280
Data subcarriers	DL: 720, UL: 560
Subcarriers/subchannel	DL: 28, UL: 24
Symbols/OFDMA frame	43

2.2. Wireless Sensor Network

The WSN is deployed in a rectangular grid and provides information about spectrum occupancy in the area where the secondary network is deployed. Each sensor senses all the primary frequency bands. Furthermore, the sensors are energy detectors. Therefore the WSN needs to synchronize quit periods with the secondary system, which are time periods of a certain length with certain intervals in between when the secondary system stops transmitting and the sensors senses primary activity. The WSN communicates its sensing result to the FC responsible for allocating frequencies to the secondary system.

Since the primary mobile WiMAX network is a slotted system with periodic MAC frames of 5 milliseconds where signals are transmitted irrespective of PU activity due to management traffic, the WSN uses real-time local sensing outcomes generated for each OFDMA frame during the sensing period. After the sensing period, the maximum received signal strength from these sensing results is reported to the FC. Sensing periods of 30 milliseconds are scheduled at specific time intervals each 0.5th second. Each sensor measures activity on all potential channels for use by the secondary system. A common control channel is used for reporting sensing measurements.

2.3. Fusion Centre

The FC collects information from the sensors and will at any time have a near real-time overview of the spectrum occupancy for the area covered by the WSN. Upon spectrum request from the secondary system, the FC uses an algorithm that consults a matrix containing spectrum usage measurements for all potential channels from all sensors in order to allocate available channels to the secondary system. Each matrix element represents a sensor in the WSN. Required functions for receiving sensor reports, calculating the spectrum map, managing allocations and communicate with the secondary system are implemented in the FC. The channel allocation algorithm allocates one of the available channels not used by the primary system.

2.4. Secondary System

The secondary system is also based on WiMAX and the ns-2 simulator model developed in WiMAX Forum. The simulator model is modified with new functionality required for operation as a secondary cognitive radio system. A centralized secondary network is considered consisting of a secondary BS and a set of SUs. The secondary system communicates with the FC in order to obtain a vacant channel for communication.

Two main cognitive functions are implemented in the secondary system. The first is a cognitive actuation module that communicates with the FC to obtain an available frequency allocation and thereafter actuates this in the secondary system. The second is time synchronization with the WSN for quiet periods during which the WSN can measure primary activity.

For the cognitive actuation module, the secondary BS communicates with the FC to obtain an available frequency for its coverage area and informs the SUs about the operating frequency. The BS is not aware of the SU coverage area and therefore the SU also queries the FC if the allocated frequency is available for it. If the frequency is not available for one of the SUs, the affected SU notifies the BS which queries the FC for a new frequency.

3. NETWORK MODEL

The considered network scenario is illustrated in Figure 2, where the primary network uses hexagonal cells without sectorization. There are totally 7 frequencies from *F1* to *F7* in the 2 GHz band. The primary network operator uses totally 70 MHz, 7 bands of 10 MHz. The secondary system consists of one BS cell co-located with one of the primary BSs illustrated by the BS with two antennas in Figure 2. The secondary BS and its SUs will use one of the frequencies *F2-F7* if available, where *F1* not will be used because the primary BS and PUs of that cell will be within interference range. Both primary and secondary BS and subscriber station heights are set to 30 and 1.5 meters respectively. The distance between primary BSs is 2 km and with hexagonal shaped cells the radius is 1.15 km. It is assumed that the primary system is noise limited. There are 65 sensors/km^2 [5]. In the remainder of this section we estimate simulation parameters to be used for this scenario.

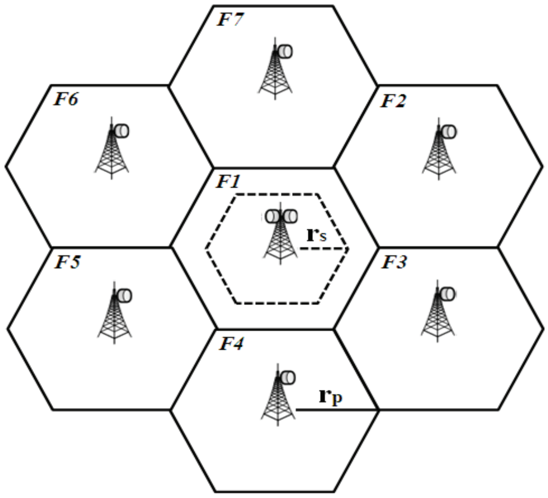

Figure 2 Network Design

3.1. Channel and Path Loss Model

The COST Hata model [15] is valid for distances above 1 km and the Cost Walfish-Ikegami (WI) [15] for distances above 20 m, and both models are valid for the 2 GHz frequency band. A path loss model which agrees with the COST-WI line-of-sight model for short distances d and with the COST Hata model at distance above 1 km is used:

$$a = P_L^{WI}(1km)$$

$$b = P_L^{Hata}(1km)$$

$$P_L(d) = \begin{cases} P_L^{WI}(d) + d(b-a), & d < 1km \\ P_L^{Hata}(d), & d \geq 1km \end{cases} \quad (1)$$

The COST Hata model is defined as:

$$P_L^{Hata}(d) = 46.3 + 33.9log_{10}(f_c) - 13.82log_{10}(h_t) - a(h_r) + \left(44.9 - 6.55log_{10}(h_t)\right)log_{10}(d) + C_M$$

where d is the distance in kilometers, f_c is the center frequency in MHz, h_t and h_r are BS and subscriber station height in meters respectively, C_M is a correction factor dependent on surrounding areas (3 for metropolitan and 0 for suburban area), $a(h_r) = (1.1\log_{10}(f_c) - 0.7)h_r - (1.56\log_{10}(f_c) - 0.8)$ is the correction factor for a medium sized city.

The COST-WI LOS model is defined as:

$$P_L^{WI}(d) = 42.6 + 26\log_{10}(d) + 20\log_{10}(f_c)$$

The channel model implemented in the OFDMA module in the ns-2 simulator is the path loss model described above combined with a Clarke-Gans implementation of Rayleigh Fading. Doppler effects are included to capture effects of node mobility and fast fading is included by modeling the channel as a Rayleigh fading channel with multiple taps as described by the ITU Pedestrian A model [16]. The path loss component is computed during simulation whereas the fast fading is computed prior to simulation.

Interference modelling in the ns-2 simulator is done at the subcarrier level by capturing packets from all transmitters in the system, both from secondary and primary nodes. When the received signal to interference plus noise ratio (SINR) on each subcarrier is calculated for each packet, a decision is made to further process or drop the packet. This is done by first finding the EESM (exponential effective SIR mapping) [17] to get the effective SINR and then extracting the block error rate (BLER) from the SINR, modulation and coding rate and block size. Based on the BLER value a decision is made whether to drop the packet or not. Please refer to [13] for details on the OFDMA implementation and interference modelling.

3.2. Primary System Transmit Power

The required transmit power P_t for the primary BS with antenna gain G_t when transmitting to a PU with antenna gain G_r at cell edge of a cell with radius r_p, is given by:

$$P_r = P_t + G_t + G_r - P_L(r_p) - X, \qquad (2)$$

where $P_L(r_p)$ is the estimated path loss between BS and PU at cell edge with Eq. (1) and X is a gaussian distributed random variable with zero mean and standard deviation of 8 dB representing shadow fading.

The primary system uses QPSK modulation and forward error correction (FEC) coding rate 1/2, which requires a minimum received signal to noise ratio (SNR) $\frac{C_r}{N} = 2.46$dB. The primary system is assumed to be designed to have a cell edge coverage of 75%, which approximately corresponds to area coverage of 90% [18]. The required received power at the PU is then:

$$P_r^{dBW} = \left(\frac{C_r}{N}\right)^{dB} + N^{dB} = \left(\frac{C_r}{N}\right)^{dB} + 10log_{10}(kTB) \qquad (3)$$

where B is the bandwidth in Hz, k the Boltzmann constant and T the temperature in Kelvin.

The average path loss at cell edge is found by using Eq. (1) with center frequency $f_c = 2$ GHz, BS height $h_t = 30$ m, PU height $h_r = 1.5$ m and correction factor $C_M = 0$ since a medium sized city is considered, to be $P_L(1.15) = 139.9$dB. The temperature is $T = 300$ K and utilized bandwidth is $B = 9189.6$ kHz. Due to limitations in the simulator, only omni-directional BS and user terminal antennas can be used. We therefore assume that both the BS and PU antenna gains are 0 dBi respectively. As a result, the calculated transmission powers will be larger than in a real scenario with directional antennas. With $G_t = 0$ dB and $G_r = 0$ dB, transmit power for the primary BS and the PU is:

$$P_t = P_L(r_p)^{dB} + X^{dB} + \left(\frac{C_r}{N}\right)^{dB} + 10log_{10}(kTB) = 13.5\ dBW. \qquad (4)$$

3.3. Sensor Threshold for Detecting the Primary Transmitters

In [19] it was required that a single sensor must be able to detect a user terminal with a probability of 0.95 (since there are many sensors the overall probability of detection will be higher). Assuming shadow fading with a standard deviation of 8 dB, the required shadow fading margin for 95% probability of detection is 13.16 dB. The threshold is then given by:

$$Threshold = P_t^{dB} - P_L(r_{ws})^{dB} - 13.16dB, \qquad (5)$$

where r_{ws} is the wireless sensing radius. With 65 sensors/km^2 [5] each sensor covers an area of 1/65km^2. Each side in the rectangle is $0.5/\sqrt{65} * \sqrt{2} * 1000$ meter and hence each sensor must cover a cell with radius $r_{ws} = 87.7$ meter. By symmetry, both the BS and PU transmit power as found in Eq. (4) should be 13.5 dBW, so the threshold is:

$$Threshold = 13.5dBW - 82.8dB - 13.16dB = -82.5\ dBW \qquad (6)$$

3.4. Requirement for Allowing Secondary Operation

In the simulator, the FC is responsible for allocating channels to the secondary system. A secondary BS or SU request a channel from the FC by sending its location and transmit power. The FC then calculates the interference range r_{int} for the querying SU as the minimum distance beyond which the generated interference is below a given limit [10]-[12]. Next, the FC checks if the received power for all sensors within r_{int} of the querying SU is below the threshold found in Eq. (6). If positive, the channel is reported as available for the SU. The interference limit used for calculating r_{int} is determined as follows:

> *The interference generated to the primary system shall correspond to an increase of the noise-floor by less than 0.5dB with a 90% probability.*

which corresponds to a shadow fading margin of 10.3 dB. The interference range r_{int} thus satisfies:

$$P_t^{dB} - P_L(r_{int})^{dB} + 10.3dB = 10log_{10}(kTB) + 10log_{10}(10^{\frac{0.5}{10}} - 1), \quad (7)$$

and the FC can now find the interference radius of the querying SU r_{int} as a function of P_t, $r_{int}(P_t)$, by using Eq. (2).

4. SIMULATION SETUP

4.1. Simulation Scenario and Cases

The main goal of this study is to find the optimal cell size for the secondary system when considering results from the business case analysis in [5], feasible deployment scenarios and the functionality of the total SENDORA system. Therefore three main cases with different cell sizes for the secondary system r_s will be considered, while primary cell size is $r_p = 1.15$ km:

a. $r_s = r_p = 1.150$ km
b. $r_s = \frac{2r_p}{3} = 0.767$ km
c. $r_s = \frac{r_p}{2} = 0.575$ km

In case (a), theoretically 100% of the secondary BSs will be co-located with a primary BS, in (b) only 11.1% and in (c) 25%. Using the number of new sites into the business cases given in [5] for cases (b) and (c) will give negative business cases, however it should be argued that the smaller cells could require less complex and less expensive BS equipment and potentially also less expensive site costs. Even though the co-location factor of case (b) is smaller than that of case (c), the latter case will require more BSs to be deployed which also will give higher costs.

4.2. Simulation Parameters

Table 2 gives the selected values for the simulation and traffic setup. Constant bit rate (CBR) traffic is transmitted in the downlink (DL) for both the primary and secondary systems. Each simulation is run 15 times, with a duration of 500s and warm up time of 20s. The results are averaged.

Table 2 Selected simulation parameters

Parameter	Primary System	Secondary System
Traffic / node	DL CBR: 0.2 Mbps	DL CBR: 1Mbps
Packet size	1500 Bytes	1500 Bytes
Nodes per BS	4	4
Node location	Random	Random
Node mobility	Rand. waypoint, rand. speed 1-20m/s	No
Cell radius (km)	1.15	0.575, 0,767, 1.15
Tx (dBW)	13.5	-40, -35, ... ,-5
Modulation/FEC	QPSK ½	QPSK ½

5. ANALYSIS OF SERVICE RANGE AND COVERAGE FOR THE SECONDARY SYSTEM

5.1. Secondary System Service Range

To get an indication of coverage we estimate the secondary system service range when using QPSK ½, which requires a minimum $\frac{C_r}{N} = 2.46$dB. We want to find the secondary cell radius r_s when having 75% coverage at cell edge where required shadow fading margin is 5.39 dB. This will approximately correspond to an area coverage of 90%. r_s must satisfy:

$$P_t - P_L(r_s) - 5.39dB = 10log_{10}(kTB) + \left(\frac{C_r}{N}\right)^{dB} \quad (8)$$

Eq. (2) is used to find a function $r_s(P_t)$ for the estimated secondary coverage r_s as a function of P_t. The estimated range of the secondary system is plotted with stippled line together with interference range in Figure 3(a). It can be observed that similar cell size of the primary and secondary systems will be difficult to achieve, at least with high probability of coverage at cell edge with transmit power 13.5dBW. Hence, the secondary system must use much lower transmission powers than the primary system which results in much lower coverage if the same cell size as for the primary system is used.

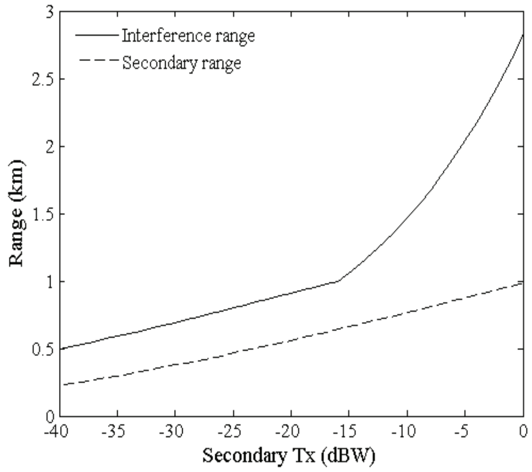

(a) Secondary service- and interference range

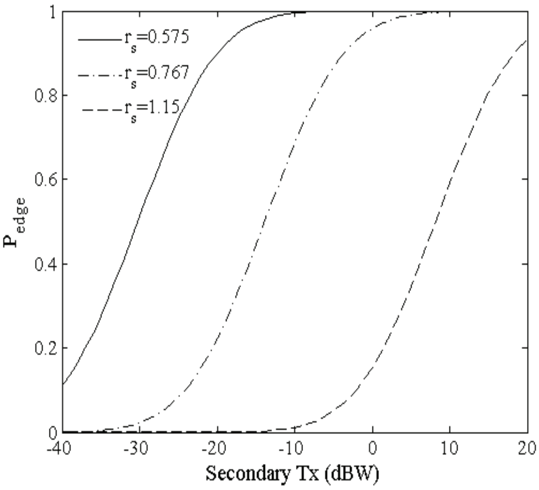

(b) Probability of coverage at cell edge

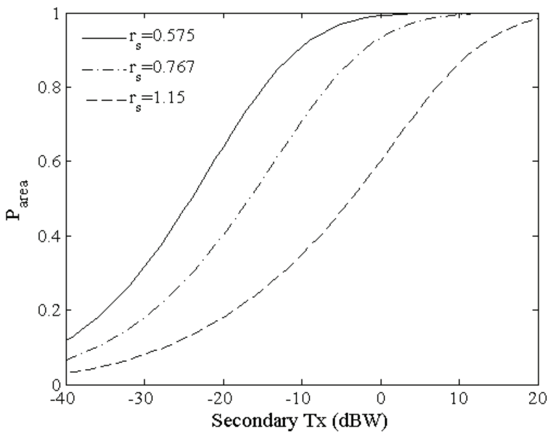

(c) Probability of area coverage

5.2. Probability of Coverage at Cell Edge

The probability of coverage at cell edge $P_{edge}[P_r(r_s) > P_{MIN}]$, where $P_{MIN} = 10\log(kTB) + \left(\frac{C_r}{N}\right)^{dB}$ is the minimum required receiver threshold and σ is the standard deviation for shadow fading, is given by:

$$P_{edge}[P_r(r_s) > P_{MIN}] = Q\left(\frac{P_{MIN} - \overline{P_r(r_s)}}{\sigma}\right) = \frac{1}{2} - \frac{1}{2}erf\left(\frac{P_{MIN} - (P_T - P_L(r_s))}{\sigma}\right) \quad (9)$$

where $\sigma = 8$dB and $\left(\frac{C_r}{N}\right)^{dB} = 2.46$dB (QPSK 1/2).

Probability of coverage at cell edge as a function of transmitted power P_t is plotted in Figure 3(b) for secondary system radius $r_s = 0.575$km and $r_s = 1.15$km, If we compare Figure 3(b) with Figure 3(a) it can be seen that it will be difficult to obtain good coverage at the cell edge for a secondary system with cell radius equal to that for the primary system cell. It can also be seen that if we reduce the secondary cell radius to half the primary cell radius, it is more likely that we are able to offer a service within that cell. However, this is also dependent on the level of interference from the primary system which also depends on the location of the primary users.

5.3. Probability of Area Coverage

When assuming a random location of the secondary nodes within the secondary cell, the probability of obtaining coverage in the cell, referred to as probability of area coverage:

$$P_{area}[P_r(r_s) > P_{MIN}] = \int_0^{r_s} Q\left(\frac{P_{MIN} - \overline{P_r(r_s)}}{\sigma}\right)\frac{2\pi r}{\pi {r_s}^2}\,dr \quad (10)$$

$$= \frac{2}{{r_s}^2}\int_0^{r_s} Q\left(\frac{P_{MIN} - (P_T - P_L(r_s))}{\sigma}\right) r\,dr$$

where r_s is the cell edge coverage radius of the secondary system. The probability of area coverage is plotted in Figure 3(c). Again, if we compare with Figure 3(a), it can be seen that there is high probability that coverage can be obtained for $r_s = 0.575$ km, but that it will be more difficult with $r_s = 1.15$ km.

6. PERFORMANCE EVALUATION AND SIMULATION RESULTS

6.1. Evaluation of Optimal Cell Sizes for the Secondary System

6.1.1 Performance of Secondary System

Average cell throughput measured at the transport layer for the secondary system for the studied cases is plotted in Figure 4(a) and the average number of SUs that obtained connectivity in Figure 4(b).

Maximum cell throughput was found to be close to 3Mbps. A lower throughput is observed for the lower transmit power levels for all three cases which is due to the lower probability of obtaining connectivity as illustrated in Figure 4(b). It can also be observed that in the cases with larger cell radius a lower percentage of the SUs obtain connectivity since the probability of being located at greater distances from the BS is higher, hence the throughput is lower. This is also confirmed by the analysis in Section 5.3. It should be noted that since the management traffic is communicated with BPSK modulation and FEC rate ½ the SUs might still obtain connectivity, but that the SNR can be to low to obtain service connectivity with QPSK ½.

Second it can be observed that the throughput reduces dramatically between -14 and -10 dBW for all three cases, which is because the probability of obtaining an available channel reduces since the interference range is higher for these higher transmit power levels. The case with $r_s = 1.15$ do never obtain maximum throughput, whereas the other two cases does. This points in the direction of shorter range and smaller and less expensive BSs for the secondary system such as WiFi access points and femto-cells.

The average number of channel switches during the simulations plotted in Figure 4(c) increases when interference range approaches the average distance between primary BS and PUs, and decreases rapidly when the probability of obtaining an available channel is reduced due to high interference range and hence there are no available channels.

6.1.2. Impact on Primary System

Average throughput measured at the transport layer for the primary system is plotted in Figure 5(a). It can be seen that the throughput is quite stable for low secondary transmit power levels, but that throughput decreases more for high secondary transmit power levels. Also, a higher throughput reduction is in general observed for the cases with larger radius which is because the SUs are closer to the PUs leading to more severe interference. It should be noted that the primary system uses retransmissions to deal with channel errors and packet loss on the physical layer, hence the throughput does not explain the whole impact on the primary system.

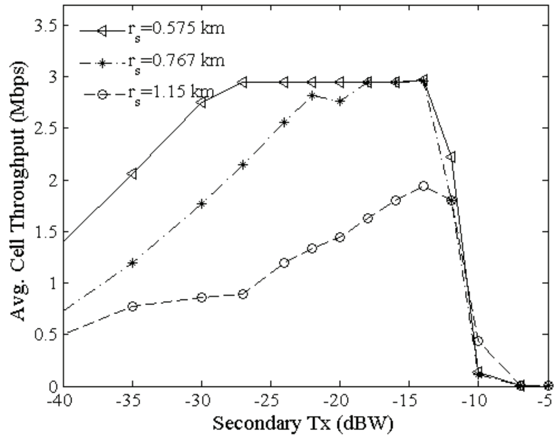

(a) Avg. cell throughput of secondary system

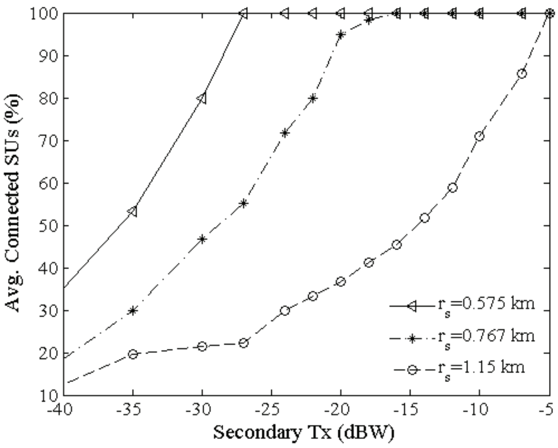

(b) Average percentage of connected SUs

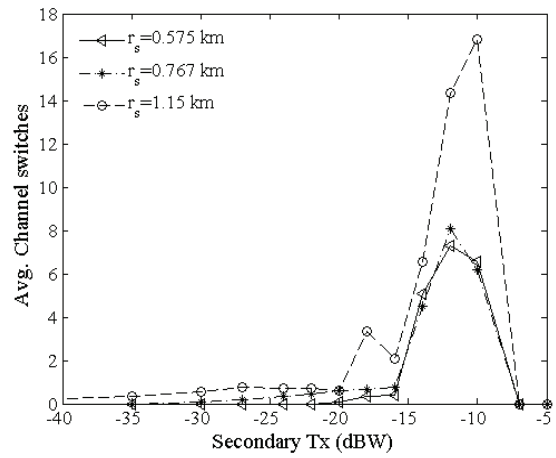

(c) Average number of channel switches

Figure 4 Performance of the secondary system

Average percentage of packet loss for the primary system is given in Figure 5(b), which shows that packet loss increases as secondary transmit power increases. Also, it can be seen that packet loss is about 50% lower for the case with $r_s = 0.575$ than the cases with larger radius. Another observation is that packet loss increases as the amount of channel switches (Figure 4(c)) in the secondary system increases, which is because there is some interference when a PU is within interference range but not yet detected due to intervals between sensing periods. Average packet loss per user does not exceed 1.8% which can be acceptable for best effort services in the primary system, but the performance of guaranteed bitrate remains to be tested.

Simulations were also run with traffic load 0.4Mbps to each PU, but the impact on both primary and secondary system throughput and packet loss was similar as presented for 0.2 Mbps.

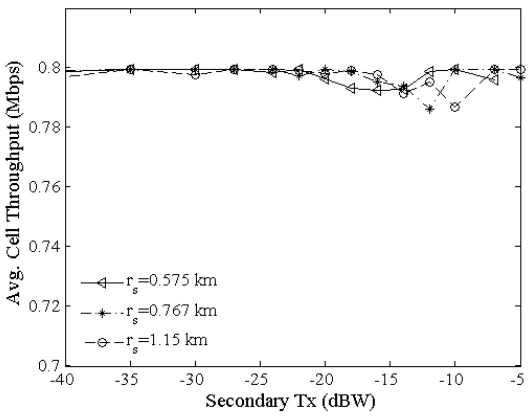

(a) Avg. cell throughput of primary system

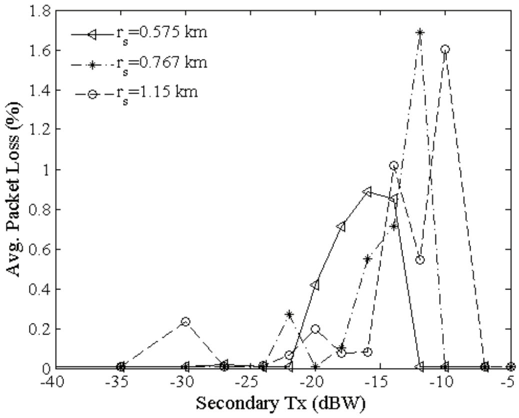

(b) Avg. Packet loss for PU

Figure 5 Impact on performance of primary system

6.2. Evaluation of Increased Load in the Secondary System

To evaluate the impact of increased load in the secondary system, we focus on the case with $r_s = 0.575$km and run additional simulations for 8 and 12 PUs. Figure 6 plots throughput measured at the transport layer for these three cases. A first observation is that throughput for cases with more SUs drops for lower transmit power levels since the probability that a PU is within interference range of a SU increases as the number of SUs increases. A second observation is that maximum throughput is reduced since more of the resources are needed for management traffic at the link layer when the number of SUs increases. No major differences were observed with respect to packet loss nor on the impact on primary system performance. Third, the cell throughput is higher for the lower transmit power levels for cases with more SUs, which is because the probability increases that a sufficient number of SUs have a connection with SNR higher than the minimum SNR of 2.46dB.

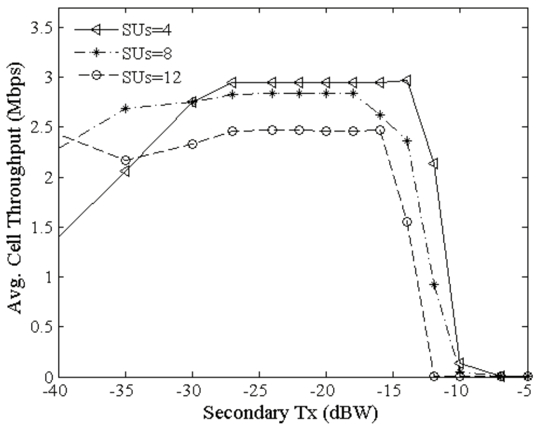

Figure 6 Secondary system throughput for increasing number of PUs

7. CONCLUSION

This paper aimed at finding the optimal cell size of the secondary system in an example SENDORA system when considering prior business case analysis, feasible deployment scenarios and the functionality of the total SENDORA system. Especially, secondary system performance and impact on the primary system was determined through simulations. First, it was found that equal cell size for the secondary and primary systems with a cellular reuse pattern with seven frequencies is difficult to achieve. This contradicts to some extent with results obtained in a prior business case analysis where co-location of secondary and primary BSs was shown to be very important in order to achieve a positive business case.

Second, it was found that a good service could be offered with secondary cell size set to half the primary cell size and with restricted transmit power levels. The number of BSs installed will then be quadrupled and at least 75% of these would not be co-located with primary BSs leading to increased costs. This points in the direction of shorter range, smaller and less expensive BSs for the secondary system such as WiFi access points and femto-cells.

For further work, considering the above findings, it will be important to study alternative deployment scenarios such as cell sectorization and real deployments with non-hexagonal cells. Second, it will be interesting to study how a relaxed requirement to allow secondary operation will impact performance. Also, since the WSN is aware of the location of primary nodes, the requirement to allow secondary operation could be relaxed dynamically in situations where primary nodes have good connectivity. Finally, adaptive dynamic transmit power for the secondary system could increase performance.

ACKNOWLEDGEMENT

Part of the research leading to these results was performed in the SENDORA project (FP7/2007-2013, under grant agreement n^{o} 216076).

REFERENCES

[1] "SENDORA project." [Online]. Available: http://www.sendora.eu/

[2] V. Fodor et al., "Sensor networks for cognitive radio: Theory and system design," in ICT Mobile Summit, Stockholm, Sweden, Jun. 10–12, 2009,

[3] FCC, "ET Docket No. 10-237," Notice of Inquery, November 30 2010.

[4] A. Hayar et al., "Performance of sendora networks," SENDORA Report, January 2011.

[5] O. Grøndalen, M. Lähtenooja, and P. Grønsund, "Evaluation of business cases for a cognitive radio network based on wireless sensor network," Accepted to IEEE DySPAN 2011, Aachen, Germany, May 3–6, 2011. [Online]. Available: http://bit.ly/hU6HYU

[6] E. Axell, E. G. Larsson, and D. Danev, "Capacity considerations for uncoordinated communication in geographical spectrum holes," Physical Communication, vol. 2, no. 1-2, pp. 3 – 9, 2009.

[7] N. Hoven and A. Sahai, "Power scaling for cognitive radio," in International Conference on Wireless Networks, Communications and Mobile Computing, vol. 1, 2005, pp. 250 – 255 vol.1.

[8] E. Larsson and M. Skoglund, "Cognitive radio in a frequency-planned environment: some basic limits," IEEE Transactions on Wireless Communications, vol. 7, no. 12, pp. 4800–4806, 2008.

[9] R. Tandra, A. Sahai, and S. Mishra, "What is a spectrum hole and what does it take to recognize one?" Proceedings of the IEEE, vol. 97, no. 5, pp. 824 –848, May 2009.

[10] M. Gastpar, "On capacity under received-signal constraints," in Proc. 2004 Allerton Conference, 2004.

[11] A. Ghasemi and E. Sousa, "Fundamental limits of spectrum-sharing in fading environments," IEEE Transactions on Wireless Communications, 2007.

[12] C.-X. Wang, X. Hong, H.-H. Chen, and J. Thompson, "On capacity of cognitive radio networks with average interference power constraints", IEEE Transactions on Wireless Communications, 2009.

[13] "The wimax forum system level simulator." [Online]. Available: http://code.google.com/p/ns2-wimax-awg/

[14] Standard for Local and metropolitan area networks Part 16: Air Interface for Fixed and Mobile Broadband Wireless Access Systems Amendment 2: Physical and Medium Access Control Layers for Combined Fixed and Mobile Operation in Licensed Bands and Corrigendum 1, IEEE Std. 802.16e, Apr. 2006.

[15] E. Demosso, "Digital mobile radio towards future generation systems. COST 231 Final report", European Commission, Brussels, Belgium, 1999. [Online]. Available: http://www.lx.it.pt/cost231

[16] ITU ITU-R M.1225, "Guidelines for evaluations of radio transmission technologies for imt-2000," 1997.

[17] "Effective SIR computation for OFDM system-level simulations," 3GPPTSG-RAN-1, Tech. Rep. RI-03-1370, 2003.

[18] C. Braithwaite and Mike Scott, UMTS Network Planning and Development. Elsevier, 2003.

[19] O. Grøndalen et al., "Scenario descriptions and system requirements," SENDORA Report, June 2010.